

## Study of the Superficial Modification of Sisal Fibres with Lignin, and Its Use As a Reinforcement Agent in Cementitious Composites

Plínio B. Mundim<sup>1</sup>, Rondinele A. R. Ferreira<sup>1</sup>, Leila A. C. Motta<sup>1</sup>, Mariana A. Henrique<sup>2</sup> and Daniel Pasquini<sup>2,\*</sup>

<sup>1</sup>College of Civil Engineering, Federal University of Uberlândia, Uberlândia, 38400-902, Brazil

<sup>2</sup>Chemistry Institute, Federal University of Uberlândia, Uberlândia, 38400-902, Brazil

\*Corresponding Author: Daniel Pasquini. Email: daniel.pasquini@ufu.br; danielpasquini2013@gmail.com

Received: 03 February 2020; Accepted: 25 March 2020

**Abstract:** The objective of this work was to evaluate different superficial treatments of sisal fibres employing lignin, and their use as a reinforcement agent in cementitious composites. The treatments consisted of superficially impregnating sisal fibres (S) with organosolv lignin (LO), organosolv lignin and glutaraldehyde (LOG), Kraft lignin (LK) and Kraft lignin and glutaraldehyde (LKG). The fibre modifications were verified by FTIR-ATR and SEM analyzes, and the presence of lignin on the surface of the fibres was evidenced, confirming the effectiveness of the treatments. The mechanical, thermal (by TGA) and water absorption properties of the fibres before and after the modifications were also investigated. After treatment, the modified fibres presented an expressive reduction of the water absorption and did not show significant changes in the mechanical properties when compared with the natural unmodified sisal fibre (SNAT). It was verified an increase in the thermal stability of the treated fibres which can be attributed to the insertion of lignin on the fibres. To evaluate the performance of the fibres in the cementitious composites, cement plates (CP) were produced with different treated fibres (CP-SLOG, CP-SLO, CP-SLKG, CP-SLK) and fibres without treatment (CP-SNAT). The composites were evaluated concerning to the water absorption, porosity and mechanical properties. The fractured regions were also investigated by SEM. All composites prepared showed similar values of absorption and porosity indexes. From the mechanical properties, the composites prepared with modified fibres showed a significant increase in the modulus of rupture and modulus of elasticity compared with CP-SNAT, while toughness was similar to all samples. From the SEM images, it was observed that the modified fibres immersed in the cementitious plates showed no degradation, indicating that the impregnation of lignin acted as a protective agent of the fibres. Therefore, the treatments of the fibres with lignin led to a significant improvement in the properties of the composites generating a treatment with potential for industrial application.

**Keywords:** Cementitious composites; sisal; lignin; surface modification



This work is licensed under a Creative Commons Attribution 4.0 International License, which permits unrestricted use, distribution, and reproduction in any medium, provided the original work is properly cited.

## 1 Introduction

The construction industry is always in search of materials with better properties that can serve its sector, and also that are environmentally and economically attractive. The health of workers involved in the production and the handling of cementitious materials is also an important factor in the area. In the case of cementitious composites, one of the biggest challenges is the replacement of asbestos, which is proven to be harmful to health and when inhaled can cause asbestosis, mesothelioma and lung cancer [1]. Asbestos is used as a reinforcement element in cementitious composites, and in some countries, it is used without restrictions. Many papers in literature present studies of plant-derived fibre applied to cementitious matrices replacing asbestos. Castoldi et al. [2] evaluated the study on the mechanical behavior and durability of concrete reinforced with polypropylene fibres and sisal fibres, replacing synthetic fibres. According to the authors, sisal fibre can provide the same level of residual strength as polypropylene fibre, if the dosing equivalence of each fibre is considered. Besides that, the degradation of sisal fibre was also avoided by the use of a low alkaline matrix; therefore, its use is feasible about its durability. Alves et al. [3] used sisal fibres with metakaolin to optimize geopolymer production. The authors observed that the use of this type of fibre presented itself as a practical alternative for field use, with a modulus of elasticity of 3.19 GPa, toughness of 2.09 kJ/m<sup>2</sup>, and modulus of rupture of approximately 9.3 MPa. Sisal fibre was chosen because it is a renewable, biodegradable and low-cost product, most of the time found as residue, allowing the production of economically viable composites. Other advantages like ductility and low specific weight can be mentioned to plant-derived composites [4–7].

In cementitious matrices, reinforced with low elasticity fibres, the main factor that influences tenacity, which is the total energy absorbed, is the fibre-matrix adherence [8]. A homogeneous mixture is also very important for the matrix, as reported by Godek et al. [9], Sadrmomtazi et al. [10] and Teixeira et al. [11]. Plant fibres must present good matrix adherence over time, to ensure the durability of the composite [12]. The durability of plant fibre-reinforced composites and the mechanical performance is directly related to the matrix and fibre interface, as it ensures the transmission of tensions that will be distributed to the matrix through reinforcement [13].

In cement-based composites, the greater fibre-matrix adherence is obtained through better performance in the transition zone, allowing both phases (fibre and matrix) to work together effectively. The best adherence is achieved by the reduction of porosity and the lowest concentration of portlandite (calcium hydroxide crystals) around the fibre [8]. The transition zone is formed in the interface between the matrix and the fibres, where the matrix microstructure is different; nature and size will depend on the type of fibre, the technology of production and there is alteration with the time [6–7]. The matrix-fibre interface characteristics influence the mechanisms of fibre displacing and removing [14].

One of the main challenges in the market for using cementitious composites reinforced with plant fibres is the durability of the material. Due to an aging process when in humidity, they suffer a reduction of resistance and tenacity. This process is related to the combination of fibre weakening by an alkaline attack, mineralization of fibres due to the migration of hydration products to the lumen and gap in plant cells, besides dimensional variation of fibres due to the high absorbance of humidity. These mechanisms cause a material reduction resistance post-peak [15].

For better mechanical performance and durability, avoiding composite degradation, it is needed to modify the hydrophilic character of fibres and improve its adherence with the matrix through surface treatment [12]. The physical treatments modify the structural and superficial properties of fibres without changing the chemical composition and can influence the adherence with the matrix [16]. Besides, the chemical treatments consist of using some chemical substance which will react with the plant fibres, to increase the interfacial adherence between fibre and matrix and decrease hydrophilicity [17]. Most methods present improvements in fibre mechanics properties and better adherence between fibre and

matrix. The most cited chemical treatments are alkaline treatment, acetylation, silane, acrylation, isocyanate, permanganate, impregnation [18].

Lignin is an amorphous substance with a complex three-dimensional structure that connects cellulosic fibres making a cell wall. It provides resistance to the compression of fibres as it hardens the cell wall and protects it from physical and chemical damages. They are molecules formed by aromatic units of phenylpropane and present macromolecular structure [19]. Some studies cited that coconut fibres are characterized by their hardness and durability, due to a high level of lignin, comparing to other natural fibres [20–21].

According to Mishra et al. [22] and Akpan et al. [23], the lignin has a hydrophobic character being the main driving forces for an efficient mixing a water-based system can be the attainment of equilibrium or minimization of free energy or inter-unit interactions; the inter-unit interactions are mostly non-covalent. The hydroxyl group content directly affects the ability to crosslink, hence the associative propensity of lignin.

Based on the above considerations, the objective of this work is to modify sisal fibres with different types of lignin and analyze the treatment influences in the physical, mechanical, thermal and morphological properties of the fibres. Also, to compare the physical and mechanical properties of fibre-cement plates molded with modified and non-modified sisal fibres, at 28 days curing and after 180 days of natural aging.

## 2 Materials and Methods

### 2.1 Modification of the Sisal Fibres with Lignin

Four modifications were proposed to sisal fibres (S) (supplied by the company Sisalsul Fibras Naturais Ltda.—São Paulo, Brazil), whose experimental conditions are described in Tab. 1. Initially, the process consists in dissolving 20 g of lignin (organosolv lignin [LO] or Kraft lignin [LK]) in a solution of 1500 mL of sodium hydroxide 0.1 M. This mixture was heated to 65°C then it was added 40 g of sisal fibres in the solution. In the experiments with glutaraldehyde (G), it was added 200 mL of this compound also in the solution with fibres. The mixture was kept in mechanical stirring for 60 minutes. After this period, a process was initialized, a fraction of 25 mL of hydrochloric acid (HCl) 1.0 M was added to the solution every 5 min. The process was completed with 90 min of reaction. After that, a filtration process took place to remove the fibres that were dried in an oven in approximately 100°C. The objective of using glutaraldehyde in the treatment was to promote the reticulation of lignin in the fibre surface. The use of HCl was for the condensation of lignin with the reduction of pH [24].

**Table 1:** Summary of experimental conditions for modification of sisal fibres with lignin

| Samples             | SLOG       | SLO        | SLKG  | SLK   |
|---------------------|------------|------------|-------|-------|
| Lignin type         | Organosolv | Organosolv | Kraft | Kraft |
| NaOH 0.1 M (mL)     | 1500       | 1500       | 1500  | 1500  |
| Lignin (g)          | 20         | 20         | 20    | 20    |
| Sisal fibre (g)     | 40         | 40         | 40    | 40    |
| Glutaraldehyde (mL) | 200        | —          | 200   | —     |
| Temperature (°C)    | 65         | 68         | 64    | 67    |
| HCl 1.0 M (mL)      | 150        | 150        | 150   | 150   |

### 2.1.1 Characterization of Unmodified and Modified Fibres

For analysis of scanning electron microscopy (SEM), the samples were cut in a size of approximately 10 mm and stick in a rack with carbon tape covered with gold. The images were taken in a Vega 3 equipment, from TESCAN. FTIR-ATR analyses were taken from FT-IR Frontier Single Range—MIR equipment, from Perkin Elmer, with 16 scans, with a scanning speed of  $0.2 \text{ cm}^{-1}$  in the interval of  $4000 \text{ cm}^{-1}$  to  $400 \text{ cm}^{-1}$ . The thermal gravimetric analysis (TGA) was done in a Shimadzu DTG-60H equipment, it was used an approximate 7 mg sample in aluminum pans, at a range of  $25^\circ\text{C}$  to  $600^\circ\text{C}$ , with a heating rate of  $10^\circ\text{C min}^{-1}$ , in an  $\text{N}_2$  atmosphere with a flow of  $30 \text{ mL min}^{-1}$ . The lignin samples were also analyzed by TGA.

### 2.1.2 Mechanical Test of the Fibres

Through a direct tensile test based on the method adopted by Motta et al. [4], the mechanical properties of tensile strength, strain, and elasticity modulus were obtained, using Instron 5982 testing machine, load cell 5 kN. The fibres were sticking with wood glue in a paper rack whose window had dimensions of  $15 \text{ mm} \times 15 \text{ mm}$ . This rack was placed on the machine trial grips using wood devices with sandpaper on the surface to ensure a better adherence and after had its sides cut, so that the tensile test would be done only in the fibres. For each treatment, 30 samples were tested, including natural fibres.

### 2.1.3 Humidity Absorption of the Fibres

A comparative evaluation was made in terms of humidity absorption between the different treatments applied to sisal fibres, according to standard ASTM E104-02 [25]. Three samples of each treatment with an approximate mass of 1.0 g were placed in a desiccator with a saturated solution of Zinc Sulfate ( $\text{ZnSO}_4$ ) to create a high humid atmosphere (99%). The test was performed in an environment with a controlled temperature similar to  $21^\circ\text{C}$ . The mass measurements were conducted in an analytical balance with a resolution of 0.00001 g, and the absorption was determined according to Eq. (1).

$$A_f = \left( \frac{m_{f,t} - m_{f,0}}{m_{f,0}} \right) 100\% \quad (1)$$

Being:  $A_f$  = fibre absorption;  $m_{f,t}$  = mass of the fibre measured at time t, in grams;  $m_{f,0}$  = initial mass of fibre, in grams.

## 2.2 Preparation of the Cementitious Composites

The preparation of composites was carried out by simulation of the Hatschek process. Cement plates (CP) were molded, with a dimension of  $20 \text{ cm} \times 20 \text{ cm} \times 0.4 \text{ cm}$ ; adding 3% of sisal fibres in volume (fibre content were fixed based on previous studies, which facilitated both the treatment of fibres and the molding of composites), also 2% of bleached Kraft eucalyptus pulp concernig the volume, minimum value to retain the cementitious material during water suction. The CPV cement was used (a cement without mineral admixture). The sisal fibres were cut with a length of 30 mm, according to the work proposed by Motta et al. [4], therefore, the matrix reinforcement is classified as discontinuous (short) and randomly oriented. The plates curing process was made in a humid chamber with a relative humidity of 75% and a temperature of  $23^\circ\text{C}$  during 28 days. After this period, the plates were cut in smaller sample parts, with dimensions of  $4 \text{ cm} \times 20 \text{ cm} \times 0.4 \text{ cm}$ . Some samples were tested at 28 days and others were subjected to natural aging in an outside environment to 180 days, in the meteorology station in the Federal University of Uberlândia, disposed into a rack with a declivity of 30%.

### 2.2.1 Microstructural Analysis of the Composites

The SEM analyses were performed on the composites after the bending tests, in the fracture regions, at 28 and 180 days. The samples were cut to 1 cm size and stuck onto the rack with carbon tape and then covered with gold. The images were purchased from Carl Zeiss, EVO MA10.

### 2.2.2 Bending Tests of the Composites

Following the procedures of Souza et al. [26], the samples were submitted to bending tests in 4 points. An Instron 5892 machine and a load cell of 5 kN were used. The span was of 150 mm e the deflection in the center of the span was measured with an Instron LVDT with a 5 mm course. The samples were tested in natural air at equilibrium moisture content. The specimens were subjected to bending tests at the ages of 28 and 180 days to determine the flexural strength, elasticity modulus, and toughness of composites. Six specimens were tested for each formulation at each age.

The toughness of the composite was determined by fracture energy ( $\text{N m m}^{-2}$ ). The specific energy was calculated from the area under the load-deflection curve divided by the cross-sectional area of the specimen. The Modulus of Rupture and Modulus of Elasticity were determined as in Eqs. (2) and (3), respectively.

$$\text{MOR} = \left( \frac{P_{\text{m\acute{a}x}} \times L}{b \times e^2} \right) \quad (2)$$

$$E = \left( \frac{23 \times L^3 \times P}{1296 \times I \times \delta} \right) \quad (3)$$

Being:  $P_{\text{m\acute{a}x}}$  = maximum force during the test (N);  $L$  = span (mm);  $b$  = width of the specimen (mm);  $e$  = thickness of the specimen (mm);  $I$  = moment of inertia of the cross section ( $\text{mm}^4$ );  $P/\delta$  = angular coefficient of the line obtained by the curve  $P \times \delta$  in the elastic stretch ( $\text{N}\cdot\text{mm}^{-1}$ ); MOR = Modulus of Rupture (MPa);  $E$  = Modulus of elasticity (MPa).

### 2.2.3 Water Absorption and Porosity of the Composites

The water absorption and the porosity of composites were determined according to standard ASTM C948-81 [27], by Eqs. (4) and (5), respectively. To determine the sample masses, the samples were submerged in water until mass stability. For a saturated dry surface mass ( $m_{\text{sss}}$ ), the sample was removed from the water, then the superficial humidity was dried, and the mass was determined in a digital balance. The immersed mass ( $m_i$ ) was determined by a hydrostatic balance. For the dry mass ( $m_s$ ) determination, the samples were dried in an oven with a temperature around  $105^\circ\text{C}$  during the minimum period of 24 h until mass stability. After removal from the oven, they were cooled in a desiccator until room temperature. With the data of immersed mass, dry surface saturated mass and dry mass, the apparent specific mass was also obtained in the samples as shown in Eq. (6).

$$\text{Ab}_c = \left( \frac{m_{\text{sss}} - m_s}{m_s} \right) \times 100\% \quad (4)$$

$$\eta = \left( \frac{m_{\text{sss}} - m_s}{m_s - m_i} \right) \times 100\% \quad (5)$$

$$\rho = \left( \frac{m_s}{m_{\text{sss}} - m_i} \right) \quad (6)$$

Being:  $\text{Ab}_{\text{cp}}$  = absorption of composites (%);  $\eta$  = porosity of composites (%);  $\rho$  = apparent specific mass of composites ( $\text{kg dm}^{-3}$ ).

## 2.3 Statistical Treatments

The results were submitted to analysis of variance and Tukey test, with a confidence level of 95% ( $p < 0.05$ ), to verify the significant differences between the average values of the mechanical properties of the fibres and the composites.

### 3 Results and Discussions

#### 3.1 Analysis of Unmodified and Modified Fibres

The SEM images presented in Fig. 1, show that the unmodified natural sisal fibre (SNAT) presented a smooth and homogeneous aspect, while SLOG, SLO, SLKG, and SLK, presented roughness and deposition of a superficial layer of lignin on the fibres, confirming that the treatment with lignin was effective.

It is known that surface roughness is one of the factors that can benefit the adherence between reinforcement and matrix. It was also observed that the integrity of the fibres was kept after the treatment.

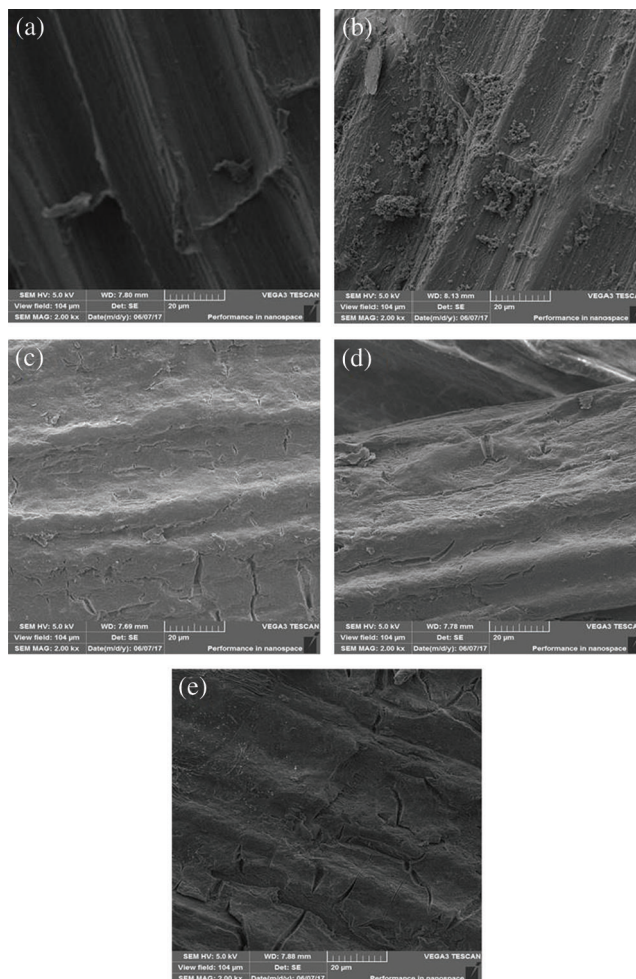


**Figure 1:** SEM images of the fibres: (a) SNAT; (b) SLOG; (c) SLO; (d) SLKG; (e) SLK. Magnification 2,000X

By the FTIR-ATR spectra presented in Fig. 2, the incorporation of lignin in the surface of the fibres can be confirmed in  $1514\text{ cm}^{-1}$  peaks which can be assigned to the C=C connection of aromatic rings, and also to the peak around  $1456\text{ cm}^{-1}$  which is related to the asymmetrical deformation of the aliphatic C-H. The peak around  $1720\text{ cm}^{-1}$  present in SNAT fibre is only observed in fibres SLOG and SLKG, probably because of the presence of non-reacted glutaraldehyde residues that were incorporated in the surface of fibres with the lignin, in fibres SLO and SLK this sign was reduced. FTIR-ATR data proves the additional presence of lignin in the fibres, corroborating with the images from SEM. Although the presence of free glutaraldehyde in the

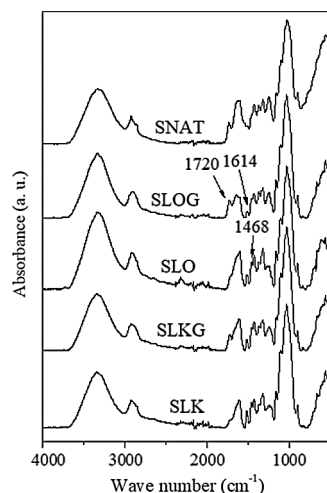


**Figure 2:** FTIR-ATR spectra of sisal fibres

fibres was detected by FTIR-ATR, it was not possible to observe the crosslinking of lignins with the fibre, which was expected with the use of glutaraldehyde.

Fig. 3 presents the curves of thermogravimetric analysis (TGA) of the fibres and lignins. To lignin, it is verified a wide range of degradation starting at around 180°C and extending to 400°C and even higher temperatures, this characteristic is due to the great thermal stability of lignins, that is already consolidated in literature. When analyzing the TGA fibre curves, it was verified that the SNAT sample presents initial degradation temperature at around 180°C, whilst for SLOG, SLO, SLKG, and SLK samples, the initial degradation temperature is around 230°C. This increase in the stability of modified fibres is due to the lignin presence, which led to an increase in thermal stability.

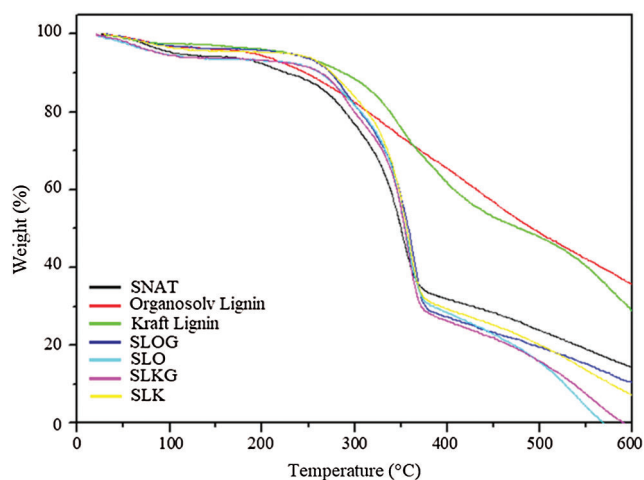


**Figure 3:** TGA curves of sisal fibres and lignins

### 3.2 Mechanical Fibre Testing (Mechanical Properties)

Tab. 2 presents the values of properties obtained in the fibres' tensile test. The displayed values show that, statistically, they did not present a significant variation between the samples. However, it is important to highlight that the chemical treatment was not detrimental to the mechanical properties of the

**Table 2:** Data of tensile strength, elasticity modulus, and strain, obtained by the direct tensile test of the fibres

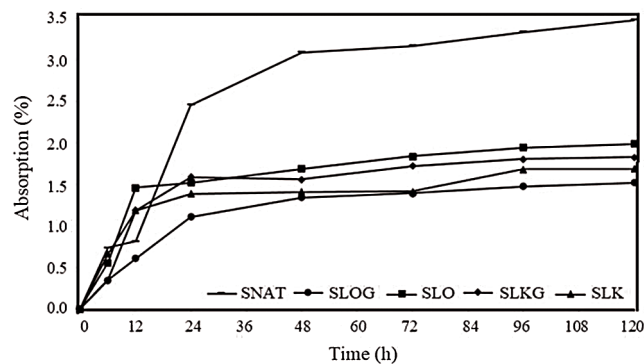
| Properties                  | SNAT                       | SLOG                       | SLO                        | SLKG                       | SLK                        |
|-----------------------------|----------------------------|----------------------------|----------------------------|----------------------------|----------------------------|
| Tensile Strength (MPa)      | 363.23<br>( $\pm 83.79$ )  | 310.58<br>( $\pm 75.20$ )  | 364.91<br>( $\pm 85.86$ )  | 355.09<br>( $\pm 96.37$ )  | 399.4<br>( $\pm 103.05$ )  |
| Modulus of Elasticity (GPa) | 11.28<br>( $\pm 2.74$ )    | 12.16<br>( $\pm 2.74$ )    | 11.32<br>( $\pm 2.81$ )    | 12.8<br>( $\pm 2.89$ )     | 11.51<br>( $\pm 1.89$ )    |
| Strain (mm/mm)              | 0.0391<br>( $\pm 0.0061$ ) | 0.0323<br>( $\pm 0.0055$ ) | 0.0417<br>( $\pm 0.0071$ ) | 0.0322<br>( $\pm 0.0075$ ) | 0.0418<br>( $\pm 0.0108$ ) |

Values in parentheses are the standards deviations. The data for each property was statistically equal.

fibres since this loss is a common situation in chemical treatments of vegetable fibres. Therefore, with the method of modification with lignin, adopted in this work, this problem could be avoided. Additionally, we can verify that the treatments with or without glutaraldehyde did not present differences in the properties of the fibres, showing that the glutaraldehyde may not have promoted the crosslinking of the lignin with the fibres as expected.

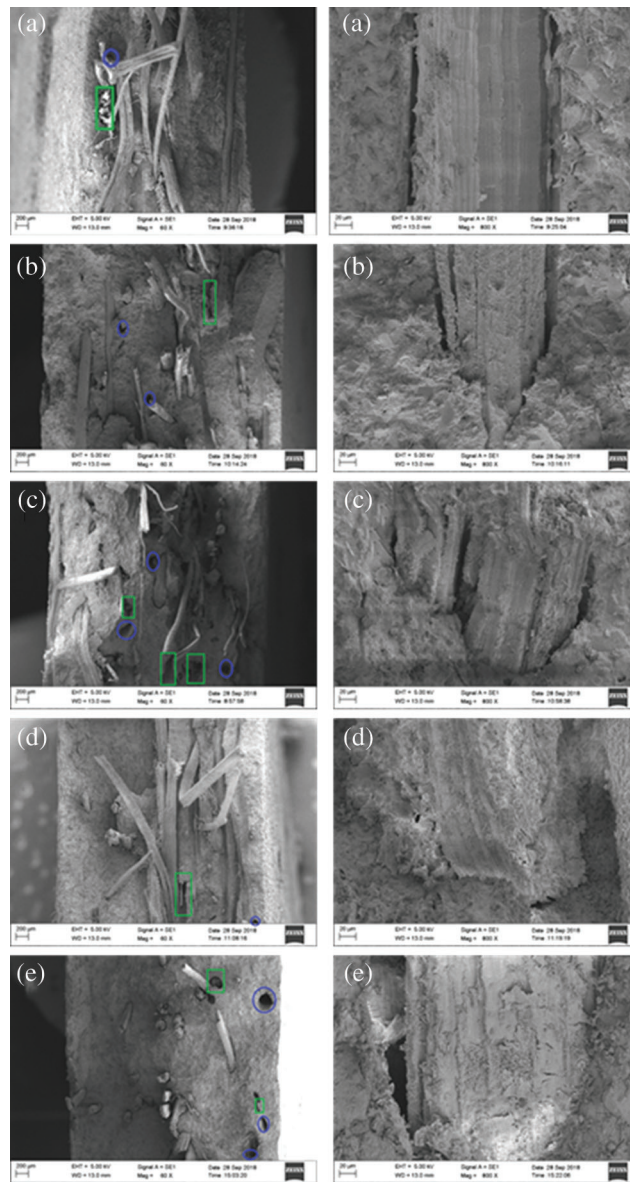
### 3.3 Humidity Absorption of the Fibres

Fig. 4 presents data obtained in the absorption test. All modified fibres presented a reduction in the final absorption, compared to SNAT, indicating that the hydrophilic character of fibres was optimized to less hydrophilic character due to the insertion of lignin. A smaller absorption in the fibres can reduce the migration of hydration products inside the fibres, aside from decrease the dimensional variation and improve the interaction between matrix and fibres [26].

**Figure 4:** Humidity absorption curves of the sisal fibres

### 3.4 Microstructural Analysis of Cementitious Composites

Fig. 5 shows SEM images of the fracture region of mechanically tested composites after aging at 180 days. It was observed the presence of regions where the fibres were pulled out and in other regions where the fibres were broken. The aging of composites contributed to the evolution of the matrix hydration, reducing porosity and improving the adhesion between the fibres and the matrix, causing the rupture of some fibres at the expense of their removal. Liu et al. [28] studied the incorporation of unmodified rice husks and modified with sodium silicate solution. They were able to observe that the modified rice husks showed a better interaction with the mortar, due to the increase of roughness, consequently a greater adhesion, improvement in the mechanical properties, and an increase in the



**Figure 5:** SEM images of the composites at 180 days: (a) CP-SNAT; (b) CP-SLOG; (c) CP-SLO; (d) CP-SLKG; (e) CP-SLK. Magnifications 60X (left) and 800X (right)

density. However, increasing rice husks content increased the number of pores in the mortar structure, resulting in decreased density and mechanical properties.

It can also be observed in Fig. 5 that the products that came from paste hydration accumulated on the surface of the fibre, once the internal structure of the fibres was not degraded even submerged in a cementitious matrix for 180 days, which indicates that the lignin impregnation treatment is protecting the fibres. Nevertheless, it was not possible to conclude by SEM images that there would have been some significant differences between the behaviors of treated fibres and non-treated before the incorporation in the cementitious matrix.

### 3.5 Bending Tests of the Composites

Tab. 3 presents data obtained in the bending tests of composites. Overall, the samples of composites produced with sisal fibres treated with lignin or with lignin and glutaraldehyde presented a higher performance than the composite prepared with natural sisal fibre. Thus, it can be verified that the treatments brought significant improvement, which can be assigned to the protective effect of lignin fibres, which acted as a barrier to the alkaline attack of fibres or as a sacrificial material preserving the fibre original structure.

**Table 3:** Values obtained in the mechanical properties of the composites

| Composites | Modulus of Rupture (MPa) |                   | Modulus of Elasticity (GPa) |                    | Toughness (kJ m <sup>-2</sup> ) |                   |
|------------|--------------------------|-------------------|-----------------------------|--------------------|---------------------------------|-------------------|
|            | 28 days                  | 180 days          | 28 days                     | 180 days           | 28 days                         | 180 days          |
| CP-SNAT    | 3.49<br>(±0.7943)        | 5.75<br>(±0.8131) | 4.21<br>(±1.0560)           | 9.18<br>(±2.0258)  | 0.35<br>(±0.0810)               | 0.45<br>(±0.1080) |
| CP-SLOG    | 9.15<br>(±1.9525)        | 9.08<br>(±1.9970) | 17.68<br>(±3.3317)          | 20.64<br>(±2.7552) | 0.75<br>(±0.1060)               | 0.44<br>(±0.0990) |
| CP-SLO     | 8.31<br>(±2.0389)        | 9.00<br>(±0.9167) | 18.15<br>(±3.1709)          | 16.64<br>(±4.3989) | 0.59<br>(±0.1230)               | 0.76<br>(±0.0970) |
| CP-SLKG    | 7.24<br>(±0.7989)        | 7.69<br>(±0.4879) | 15.79<br>(±3.4069)          | 15.16<br>(±2.7742) | 0.69<br>(±0.1390)               | 0.29<br>(±0.0480) |
| CP-SLK     | 7.28<br>(±1.3890)        | 8.00<br>(±1.7584) | 15.11<br>(±1.6806)          | 18.13<br>(±2.4481) | 0.65<br>(±0.0890)               | 0.35<br>(±0.0860) |

Values in parentheses are standard deviation.

The low porosity and better mechanical properties of composites with fibres treated are indicative that the interaction between matrix and fibre improved with treatment. This behavior has remained with aging, especially for the composite CP-SLO, which kept high the modulus of rupture and modulus of elasticity and showed significant growth of toughness.

The aging of composites increased the rigidity with consequent reduction of the toughness. This was expected by the improvement of fibre/matrix interaction by densification of the matrix, reducing the pullout, and increasing fibre rupture. However, the CP-SLO composite presented an increase in toughness, though aging, indicating that the fibres are preserved and acting as reinforcement efficiently. Through, in the untreated composites, the toughness was low at 28 days and remains low with aging.

The composites with the treated fibres presented modulus of rupture and modulus of elasticity significantly higher in the two test ages. The micrographs of the composites remark the presence of hydration products on the surface of the treated fibres, indicating that there may have been better adherence of these fibres to the matrix, resulting in composites with better performance, even after aging.

### 3.6 Water Absorption and Porosity of the Composites

Tab. 4 presents the results obtained in the absorption and porosity tests. It is known that the rates of absorption, porosity, and apparent specific mass are directly related to each other. There were a lower absorption and porosity of the samples with the treated fibres, corroborating the results of the improved mechanical properties for the composites with the treated fibres, probably by reducing the water absorption from the treated fibres and better Interface. With the aging of the composites, the porosity was

**Table 4:** Values obtained in the absorption and porosity of the composites

| Composites | Absorption (%) |           | Porosity (%) |           | Apparent specific mass (kg dm <sup>-3</sup> ) |           |
|------------|----------------|-----------|--------------|-----------|---|-----------|
|            | 28 dias        | 180 dias  | 28 dias      | 180 dias  | 28 dias                                       | 180 dias  |
| CP-SNAT    | 21.62%         | 16.24%    | 58.70%       | 40.67%    | 1.711   | 1.781     |
|            | (±0.0155)      | (±0.0128) | (±0.0481)    | (±0.0320) | (±0.0353)                                     | (±0.0494) |
| CP-SLOG    | 16.96%         | 13.58%    | 44.81%       | 33.68%    | 1.829   | 1.857     |
|            | (±0.0317)      | (±0.0176) | (±0.0846)    | (±0.0421) | (±0.1027)                                     | (±0.0725) |
| CP-SLO     | 18.10%         | 16.06%    | 47.84%       | 39.22%    | 1.792   | 1.755     |
|            | (±0.0278)      | (±0.0140) | (±0.0719)    | (±0.0326) | (±0.0896)                                     | (±0.0492) |
| CP-SLKG    | 15.86%         | 15.31%    | 41.61%       | 35.59%    | 1.853   | 1.737     |
|            | (±0.0126)      | (±0.0380) | (±0.0331)    | (±0.0765) | (±0.0432)                                     | (±0.2193) |
| CP-SLK     | 15.11%         | 14.43%    | 39.69%       | 35.93%    | 1.881   | 1.836     |
|            | (±0.0082)      | (±0.0177) | (±0.0203)    | (±0.0374) | (±0.0334)                                     | (±0.0827) |

Values in parentheses are standard deviation.

reduced by the advancement of the matrix hydration and another probable cause for reduction of the absorption indexes, and consequently of porosity is the phenomenon of carbonation [29].

#### 4 Conclusions

It was possible to observe that the incorporation of lignin was successful in all treatments studied, preserving the internal structure of the fibres, thus maintaining the original mechanical properties. The similarity shown in the behavior of fibres in all treatments leads to the belief that there was no crosslinking (reticulation) between lignin and fibres. It was possible to observe that the addition of lignin improved the properties in the modified fibres when compared to the unmodified ones.

As for the mechanical parameters for the composites, it was possible to verify that the treatments used in the fibres in this study were effective to improve these properties without modifying or impairing the integrity of the fibres. Among the treatments used, the treatments with organosolv lignin (LO) and organosolv lignin with glutaraldehyde (LOG) showed the best results for the composites. However, the presence of glutaraldehyde can be dispensed with, since its use has not shown significant differences in treatment.

Given the above, it can be concluded that the treatment of sisal fibres for cementitious composites with lignin is effective, and because it is a simple process, it has a high potential for industrial applications.

**Acknowledgement:** The authors would like to acknowledge CNPq, CAPES, FINEP and FAPEMIG for supporting this work.

**Funding Statement:** The author(s) received no specific funding for this study.

**Conflicts of Interest:** The authors declare that they have no conflicts of interest to report regarding the present work.

#### References

1. Terra Filho, M., Pde Freitas, J. B., Nery, L. E. (2006). Doenças asbesto-relacionadas. *Jornal Brasileiro de Pneumologia*, 32(suppl 2), S48–S53. DOI 10.1590/S1806-37132006000800009.

2. Castoldi, R. S., Souza, L. M. S., Silva, F. A. (2019). Comparative study on the mechanical behavior and durability of polypropylene and sisal fiber reinforced concretes. *Construction and Building Materials*, 211, 617–628. DOI 10.1016/j.conbuildmat.2019.03.282.
3. Alves, L. C. S., Ferreira, R. A. R., Machado, L. B., Motta, L. A. C. (2019). Optimization of metakaolin-based geopolymer reinforced with sisal fibers using response surface methodology. *Industrial Crops and Products*, 139, 111551. DOI 10.1016/j.indcrop.2019.111551.
4. Motta, L. A. C., John, V. M., Agopyan, V. (2010). Thermo-mechanical treatment to improve properties of sisal fibres composites. *Materials Science Forum*, 636–637, 253–259. DOI 10.4028/www.scientific.net/MSF.636-637.253.
5. Pacheco-Torgal, F., Jalali, S. (2011). Cementitious building materials reinforced with vegetable fibres: a review. *Construction and Building Materials*, 25(2), 575–581. DOI 10.1016/j.conbuildmat.2010.07.024.
6. Pickering, K. L., Aruan Efendy, M. G., Le, T. M. (2016). A review of recent development in natural fibre composites and their mechanical performance. *Composites Part A: Applied Science and Manufacturing*, 83, 98–112. DOI 10.1016/j.compositesa.2015.08.038.
7. Yan, L., Kasal, B., Huang, L. (2016). A review of recent research on the use of cellulosic fibres, their fibre fabric reinforced cementitious, geo-polymer and polymer composites in civil engineering. *Composites Part B: Engineering*, 92, 94–132. DOI 10.1016/j.compositesb.2016.02.002.
8. Savastano Junior, H., Agopyan, V. (1999). Transition zone studies of vegetable fibre-cement paste composites. *Cement and Concrete Composites*, 21(1), 49–57. DOI 10.1016/S0958-9465(98)00038-9.
9. Godek, E., Felekoglu, T., Keskinates, M., Felekoglu, B. (2017). Development of flaw tolerant fiber reinforced cementitious composites with calcined kaolin. *Applied Clay Science*, 146, 423–431. DOI 10.1016/j.clay.2017.06.029.
10. Sadrumontazi, A., Tahmouresi, B., Saradar, A. (2018). Effects of silica fume on mechanical strength and microstructure of basalt fiber reinforced cementitious composites (BFRCC). *Construction and Building Materials*, 162, 321–333. DOI 10.1016/j.conbuildmat.2017.11.159.
11. Teixeira, R. S., Santos, S. F., Christoforo, A. L., Payá, J., Savastano, H. Jr., et al. (2019). Impact of content and length of curauá fibers on mechanical behavior of extruded cementitious composites: Analysis of variance. *Cement and Concrete Composites*, 102, 134–144. DOI 10.1016/j.cemconcomp.2019.04.022.
12. Ardanuy, M., Claramunt, J., Toledo Filho, R. D. (2015). Cellulosic fiber reinforced cement-based composites: a review of recent research. *Construction and Building Materials*, 79, 115–128. DOI 10.1016/j.conbuildmat.2015.01.035.
13. Dos Santos Marques, M. G., Melo Filho, J. A., Molina, J. C., Toledo Filho, R. D., de Vasconcelos, R. P., et al. (2014). Numerical-experimental assessment of the arumã fiber as reinforcement to the cementitious matrix. *Key Engineering Materials*, 600, 460–468. DOI 10.4028/www.scientific.net/KEM.600.460.
14. Bentur, A., Mindess, S. (2006). *Fibre reinforced cementitious composites*. 2nd edition. Great Britain: Taylor & Francis. DOI 10.1201/9781482267747,
15. Ardanuy, M., Claramunt, J., García-Hortal, J. A., Barra, M. (2011). Fiber-matrix interactions in cement mortar composites reinforced with cellulosic fibers. *Cellulose*, 18(2), 281–289. DOI 10.1007/s10570-011-9493-3.
16. Faruk, O., Bledzki, A. K., Fink, H. P., Sain, M. (2012). Biocomposites reinforced with natural fibers: 2000–2010. *Progress in Polymer Science*, 37(11), 1552–1596. DOI 10.1016/j.progpolymsci.2012.04.003.
17. Albinete, S. R., Pacheco, E. B. A. V., Visconte, L. L. Y. (2013). Revisão dos tratamentos químicos da fibra natural para mistura com poliolefinas. *Química Nova*, 36(1), 114–122. DOI 10.1590/S0100-40422013000100021.
18. Li, X., Tabil, L. G., Panigrahi, S. (2007). Chemical treatments of natural fiber for use in natural fiber reinforced composites: a review. *Journal of Polymers and the Environment*, 15(1), 25–33. DOI 10.1007/s10924-006-0042-3.
19. Lin, S. Y., Dence, C. W. (1992). *Methods in lignin chemistry*. Berlin: Springer-Verlag, 10.1007/978-3-642-74065-7.
20. Ali, M., Liu, A., Sou, H., Chouw, N. (2012). Mechanical and dynamic properties of coconut fibre reinforced concrete. *Construction and Building Materials*, 30, 814–825. DOI 10.1016/j.conbuildmat.2011.12.068.

21. Ishizaki, M. H., Visconte, L. L. Y., Furtado, C. R. G., Leite, M. C. A. M., Leblanc, J. L. (2006). Caracterização mecânica e morfológica de compósitos de polipropileno e fibras de coco verde: influência do teor de fibra e das condições de mistura. *Polímeros*, 16, 182–186. DOI 10.1590/S0104-14282006000300006.
22. Mishra, P. K., Ekielski, A. (2019). The self-assembly of lignin and its application in nanoparticle synthesis: a short review. *Nanomaterials*, 9(2), 243. DOI 10.3390/nano9020243.
23. Akpan, E. I., Adeosun, S. O. (2019). *Sustainable lignin for carbon fibers: principles, techniques, and applications*. Springer, Gewerbestrasse, Switzerland, 10.1007/978-3-030-18792-7,
24. Novo, L. P., Gurgel, L. V. A., Marabezi, K., Curvelo, A. A. S. (2011). Delignification of sugarcane bagasse using glycerol-water mixtures to produce pulps for saccharification. *Bioresource Technology*, 102(21), 1040–10046. DOI 10.1016/j.biortech.2011.08.050.
25. American Society for Testing Materials—ASTM E104-02. (2012). *Standard practice for maintaining constant relative humidity by means of aqueous solutions*. ASTM, Philadelphia.
26. Souza, J. D. G. T., Motta, L. A. C., Pasquini, D., Vieira, J. G., Pires, C. (2017). Surface chemical modification of sponge gourd fiber aiming at compatibility and application as reinforcement in cementitious matrix. *Ambiente Construído*, 17(2), 269–283. DOI 10.1590/s1678-86212017000200157.
27. American Society for Testing Materials—ASTM C948-81 (2009). *Dry and wet bulk density, water absorption and apparent porosity of thin sections of glass-fiber-reinforced concrete*. ASTM, Philadelphia.
28. Liu, J. S., Li, F. P., He, X., Liu, X. F., Zhang, R. T. (2018). Experimental study in the modification of mortar samples with incorporated rice husk. *Journal of Testing and Evaluation*, 46(3), 967–973. DOI 10.1520/JTE20170027.
29. Tonoli, G. H. D., Santos, S. F., Joaquim, A. P., Savastano, H. Jr. (2010). Effect of accelerated carbonation on cementitious roofing tiles reinforced with lignocellulosic fibre. *Construction and Building Materials*, 24(2), 193–201. DOI 10.1016/j.conbuildmat.2007.11.018.